



Synthesis and characterization of some novel ruthenium(II) complexes containing thiolate ligands

Prashant Kumar, Mahendra Yadav, Ashish Kumar Singh, Daya Shankar Pandey*

Department of Chemistry, Faculty of Science, Banaras Hindu University, Varanasi 221005, UP, India

ARTICLE INFO

Article history:

Received 30 September 2009

Received in revised form 4 December 2009

Accepted 7 December 2009

Available online 13 December 2009

Keywords:

Ruthenium complexes

2-Mercapto-5-methyl-1,3,5-thiadiazole

2-Mercapto-4-methyl-5-thiazoleacetic acid

2-Mercaptobenzothiazole

Diphenyl-2-pyridylphosphine

ABSTRACT

Reactions of the ruthenium complexes $[\text{RuH}(\text{CO})\text{Cl}(\text{PPh}_3)_3]$ and $[\text{RuCl}_2(\text{PPh}_3)_3]$ with hetero-difunctional *S,N*-donor ligands 2-mercapto-5-methyl-1,3,5-thiadiazole (HL^1), 2-mercapto-4-methyl-5-thiazoleacetic acid (HL^2), and 2-mercaptobenzothiazole (HL^3) have been investigated. Neutral complexes $[\text{RuCl}(\text{CO})(\text{PPh}_3)_2(\text{HL}^1)]$ (**1**), $[\text{RuCl}(\text{CO})(\text{PPh}_3)_2(\text{HL}^2)]$ (**2**), $[\text{RuCl}(\text{CO})(\text{PPh}_3)_2(\text{HL}^3)]$ (**3**), $[\text{Ru}(\text{PPh}_3)_2(\text{HL}^1)_2]$ (**4**), $[\text{RuCl}(\text{PPh}_3)_3(\text{HL}^2)]$ (**5**), and $[\text{RuCl}(\text{PPh}_3)_3(\text{HL}^3)]$ (**6**) imparting κ^2 -*S,N*-bonded ligands have been isolated from these reactions. Complexes **1** and **4** reacted with diphenyl-2-pyridylphosphine (PPh_2Py) to give neutral κ^1 -*P* bonded complexes $[\text{RuCl}(\text{CO})(\kappa^1\text{-P-PPh}_2\text{Py})_2(\text{HL}^1)]$ (**7**), and $[\text{Ru}(\kappa^1\text{-P-PPh}_2\text{Py})_2(\text{HL}^1)_2]$ (**8**). Complexes **1–8** have been characterized by analytical, spectral (IR, NMR, and electronic absorption) and electrochemical studies. Molecular structures of **1**, **2**, **4**, and **7** have been determined crystallographically. Crystal structure determination revealed coordination of the mercapto-thiadiazole ligands (HL^1 – HL^3) to ruthenium as κ^2 -*N,S*-thiolates and presence of *rare* intermolecular *S–S* weak bonding interaction in complex **1**.

© 2010 Elsevier B.V. All rights reserved.

1. Introduction

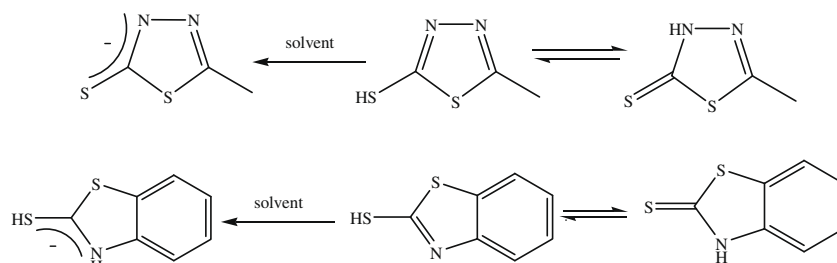
The role of organo-sulfur compounds is well documented in the chemical and biological processes [1,2]. *N*-heterocyclic thiones containing thioamide group are intriguing ligands in coordination chemistry, since these can adopt versatile coordination modes using exocyclic sulfur and endocyclic nitrogen donors (Scheme 1) [3–6]. Mercapto-substituted thiadiazoles exist in thiol and thione tautomeric forms. Also, these exhibit prototropic tautomerism, acid–base equilibrium and redox reactions based on mercapto to disulfido conversions. Tautomerization influences the reactivity of thiadiazoles and has been demonstrated in the polymerization processes [7], substitution reactions at different moieties [8,9], and in metal complexation reactions [5,6]. A variety of *N*-heterocyclic thiones having 5-membered, 6-membered and other condensed cycles have extensively been used in the synthesis of both transition and non-transition metal complexes [10–13]. Among these, 2-mercapto-5-methyl-1,3,5-thiadiazole (HL^1), 2-mercapto-4-methyl-5-thiazoleacetic acid (HL^2), and 2-mercaptobenzothiazole (HL^3) are particularly interesting. Due to presence of two donor sites in its protonated and deprotonated forms it may bind with two or more metal ions within a rather rigid and compact molecular space and promote interaction between the metal ions (Scheme 2) [14–19].

Further, large size of sulfur makes it easier to adopt different angles on coordination to metal ion in the complexes.

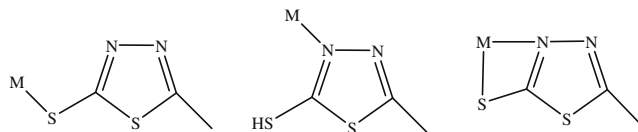
The synthetic utility of mercapto-functionalised thiadiazoles and derivatives as bio-active compounds, metal chelating agents, lubricant additives like corrosion inhibitors and anti-wear agents, cross-linkers for polymers, components of cathode material battery systems, and in the syntheses of various organic compounds has been reported [7,8,20,21]. A few platinum group metal complexes imparting thiadiazole ligands have also been reported in the literature [22,23]. Despite its extensive chemistry, reactivity of the complexes $[\text{RuCl}_2(\text{PPh}_3)_3]$ and $[\text{RuH}(\text{CO})\text{Cl}(\text{PPh}_3)_3]$ with mercapto-functionalised thiadiazoles, has not yet been explored. Because of our interests in this area we have examined reactivity of complexes $[\text{RuCl}_2(\text{PPh}_3)_3]$ and $[\text{RuH}(\text{CO})\text{Cl}(\text{PPh}_3)_3]$ with 2-mercapto-5-methyl-1,3,5-thiadiazole, 2-mercapto-4-methyl-5-thiazoleacetic acid, and 2-mercaptobenzothiazole. Further, diphenyl-2-pyridylphosphine is one of the most useful ligands applied in coordination chemistry of the transition metals. It acts as a monodentate or bidentate chelating ligand depending upon requirements of the metal centre [24–26]. We report herein syntheses, spectral, electrochemical and structural characterization of some ruthenium complexes containing mercapto-functionalised thiadiazoles in neutral chelating and diphenyl-2-pyridylphosphine (PPh_2Py) in neutral monodentate mode. Also, we describe herein crystal structures of the complexes $[\text{RuCl}(\text{CO})(\text{PPh}_3)_2(\text{HL}^1)]$, $[\text{RuCl}(\text{CO})(\text{PPh}_3)_2(\text{HL}^2)]$, $[\text{Ru}(\text{PPh}_3)_2(\text{HL}^1)_2]$, and $[\text{RuCl}(\text{CO})(\kappa^1\text{-P-PPh}_2\text{Py})_2(\text{HL}^1)]$.

* Corresponding author. Tel.: +91 542 6702480.

E-mail address: [dspbhhu@bhu.ac.in](mailto:dspbhu@bhu.ac.in) (D.S. Pandey).



Scheme 1.



Scheme 2.

2. Experimental

2.1. Materials and physical measurements

Analytical grade chemicals were used throughout. The synthetic manipulations were performed under oxygen free nitrogen atmosphere. Solvents were dried and distilled before use by standard literature procedures [27]. Hydrated ruthenium(III) chloride, 2-mercapto-5-methyl-1,3,5-thiadiazole, 2-mercapto-4-methyl-5-thiazoleacetic acid, 2-mercaptobenzothiazole, and 2-mercapto-1-methylimidazole and diphenyl-2-pyridylphosphine were procured from Aldrich Chemical Company, Inc., USA and were used without further purifications. The precursor complexes $[\text{RuH}(\text{CO})\text{Cl}(\text{PPh}_3)_3]$ and $[\text{RuCl}_2(\text{PPh}_3)_3]$ were prepared and purified following the literature procedures [28,29].

C, H and N analyses were performed on an Exeter Analytical Inc., Model CE-440 Elemental Analyzer. IR spectra were acquired on a Varian 3300 FT-IR spectrometer in the region 4000–400 cm^{-1} . Electronic absorption spectra were recorded on a Shimadzu UV-1700 spectrophotometer at room temperature. ^1H and ^{31}P NMR spectra in CDCl_3 were obtained on a JEOL AL 300 FT-NMR spectrometer at room temperature using TMS as an internal reference for ^1H and 85% H_3PO_4 for ^{31}P NMR. FAB mass spectra were recorded on a JEOL SX 102/Da-600 Mass Spectrometer. Electrochemical studies were performed on a CHI 620c Electrochemical Analyzer. A platinum working electrode, platinum wire auxiliary electrode, and Ag/Ag^+ reference electrode were used in a standard three-electrode configuration. Tetrabutylammonium perchlorate (TBAP) was used as supporting electrolyte, and the solution concentration was ca. 10^{-3} M.

2.2. Syntheses

2.2.1. Synthesis of $[\text{Ru}(\text{CO})\text{Cl}(\text{PPh}_3)_2(\text{HL}^1)]\cdot\text{CH}_2\text{Cl}_2$ **1**

To a suspension of $[\text{RuH}(\text{CO})\text{Cl}(\text{PPh}_3)_3]$ (0.5 g, 0.67 mmol) in methanol (25 mL), HL^1 (0.066 g, 0.50 mmol) was added and contents of the flask were heated under reflux for 8 h. Slowly, it gave a clear orange solution. After cooling to room temperature the solution was filtered through celite and concentrated to dryness under reduced pressure. Residue was extracted with dichloromethane (5 mL) and filtered. Diethyl ether (50 mL) was added to the filtrate, and left for slow crystallization. Slowly, it gave an orange microcrystalline solid which was separated by filtration washed with diethyl ether and dried *in vacuo*. Yield: 0.358 g, 72%.

Microanalytical data: Anal. Calc. for $\text{C}_{41}\text{H}_{35}\text{Cl}_3\text{N}_2\text{OP}_2\text{RuS}_2$: C, 54.40; H, 3.90; N, 3.09. Found: C, 54.38; H, 3.86; N, 3.06%. ^1H NMR (δ ppm): 7.36–7.02 (m, 30H, PPh_3), 2.50 (s, 3H, CH_3). $^{31}\text{P}\{^1\text{H}\}$ NMR (δ ppm): 40.72 (s, PPh_3). IR (KBr pellet, cm^{-1}): 1927 (s), 1575 (s), 1480 (s), 1433 (s), 1375 (m), 1188 (m), 1131 (s), 1090 (m), 746 (m), 696 (s), 514 (s), 280 $\nu(\text{Ru}-\text{Cl})$. UV-Vis. [λ_{max} , nm (ϵ): 483 (472), 355 (14 740), 277 (38 070), 247 (38 250).

2.2.2. Synthesis of $[\text{Ru}(\text{CO})\text{Cl}(\text{PPh}_3)_2(\text{HL}^2)]$ **2**

It was prepared from $[\text{RuH}(\text{CO})\text{Cl}(\text{PPh}_3)_3]$ (0.1 g, 0.10 mmol) and HL^2 (0.19 mg, 0.10 mmol) following the above procedure for **1**. Complex **2** separated as a yellow crystalline solid. Yield: 0.657 g, 75%. Microanalytical data: Anal. Calc. for $\text{C}_{43}\text{H}_{37}\text{Cl}_3\text{NO}_4\text{P}_2\text{RuS}_2$: C, 53.51; H, 3.86; N, 1.45. Found: C, 53.86; H, 4.16; N, 1.62%. ^1H NMR (δ ppm): 2.47 (s, 3H, CH_3), 3.49 (s, 2H, CH_2), 7.30–7.04 (m, 30H, PPh_3). $^{31}\text{P}\{^1\text{H}\}$ NMR (δ ppm): 44.82 (s, PPh_3). IR (KBr pellet, cm^{-1}): 3425 (m), 1930 (s), 1720 (s), 1576 (s), 1481 (s), 1430 (s), 1374 (m), 1182 (m), 1130 (s), 1089 (m), 746 (m), 696 (s), 518 (s), 292 $\nu(\text{Ru}-\text{Cl})$. UV-Vis. [λ_{max} , nm (ϵ): 485 (1980), 377 (14 400), 281 (37 400), 251 (37 700).

2.2.3. Synthesis of $[\text{Ru}(\text{CO})\text{Cl}(\text{PPh}_3)_2(\text{HL}^3)]$ **3**

The complex **3** was prepared following the above procedure for **1** except that HL^3 (0.17 g, 0.10 mmol) was used in place HL^1 . It was obtained as an orange microcrystalline solid. Yield: 0.572 g, 67%. Microanalytical data: Anal. Calc. for $\text{C}_{44}\text{H}_{34}\text{Cl}_3\text{NOP}_2\text{RuS}_2$: C, 61.78; H, 4.01; N, 1.64. Found: C, 61.75; H, 4.02; N, 1.63%. ^1H NMR (δ ppm): 8.61 (dd, 7.6 Hz, 1 H), 7.67 (dd, 7.8 Hz, 1 H), 7.33 (td, 7.8 Hz, 1 H), 7.24 (td, 7.6 Hz, 1 H), 7.28–7.02 (br m, PPh_3). $^{31}\text{P}\{^1\text{H}\}$ NMR (δ ppm): 39.85 (s, PPh_3). IR (KBr pellet, cm^{-1}): 1927 (s), 1670 (s), 1576 (s), 1488 (s), 1435 (s), 1372 (m), 1182 (m), 1131 (s), 1089 (m), 746 (m), 698 (s), 516 (s), 292 $\nu(\text{Ru}-\text{Cl})$. UV-Vis. [λ_{max} , nm (ϵ): 479 (1480), 373 (13 200), 329 (37 700), 253 (38 000).

2.2.4. Synthesis of $[\text{Ru}(\text{PPh}_3)_2(\text{HL}^1)_2]$ **4**

This complex was prepared using $[\text{RuCl}_2(\text{PPh}_3)_3]$ (0.1 g, 0.10 mmol) and HL^1 (0.26 g, 0.20 mmol) in methanol (25 mL) following the procedure employed for **1**. It was obtained as a yellow crystalline solid. Yield: 0.790 g, 89%. Microanalytical data: Anal. Calc. for $\text{C}_{42}\text{H}_{36}\text{N}_4\text{P}_2\text{RuS}_4$: C, 56.81; H, 4.09; N, 6.31. Found: C, 56.80; H, 4.07; N, 6.33%. ^1H NMR (δ ppm): 7.34–7.10 (br m, 30H, PPh_3), 2.38 (s, 3H, CH_3). $^{31}\text{P}\{^1\text{H}\}$ NMR (δ ppm): 42.24 (s, PPh_3). IR (KBr pellet, cm^{-1}): 1572 (s), 1482 (s), 1432 (s), 1361 (m), 1189 (m), 1136 (m), 1085 (m), 807 (m), 744 (m), 696 (s), 519 (s). UV-Vis. [λ_{max} , nm (ϵ): 409 (2990), 341 (9360), 253 (38 400).

2.2.5. Synthesis of $[\text{RuCl}(\text{PPh}_3)_3(\text{HL}^2)]$ **5**

Complex **5** was prepared following the above procedure for **4** using HL^2 (0.19 mg, 0.10 mmol) in place of HL^1 (0.26 g, 0.20 mmol). It isolated as an orange microcrystalline solid. Yield: 0.799 g, 72%. Microanalytical data: Anal. Calc. for $\text{C}_{60}\text{H}_{51}\text{ClNO}_2\text{P}_3\text{RuS}_2$: C, 64.83;

H, 4.62; N, 1.26. Found: C, 64.86; H, 4.61; N, 1.28%. ^1H NMR (δ ppm): 2.37 (s, 3H, CH_3), 3.46 (s, 2H, CH_2), 7.38–7.02 (m, 45H, PPh_3). $^{31}\text{P}\{^1\text{H}\}$ NMR (δ ppm): 59.72 (s, PPh_3), and 54.90 (s, PPh_3). IR (KBr pellet, cm^{-1}): 3425 (m), 1718 (s), 1572 (s), 1475 (s), 1429 (s), 1372 (m), 1180 (m), 1126 (s), 1092 (m), 746 (m), 695 (s), 520 (s), 298 $\nu(\text{Ru}-\text{Cl})$. UV–Vis. [λ_{max} , nm (ϵ): 476 (1672), 367 (14 200), 277 (37 200), 245 (33 500).

2.2.6. Synthesis of $[\text{RuCl}(\text{PPh}_3)_3(\text{HL}^3)] \mathbf{6}$

Complex **6** was prepared following the above procedure for **5** using HL^3 (0.17 g, 0.10 mmol). After work-up it was obtained as a yellow crystalline solid. Yield: 0.833 g, 77%. Microanalytical data: Anal. Calc. for $\text{C}_{61}\text{H}_{49}\text{ClN}_3\text{P}_3\text{RuS}_2$: C, 67.24; H, 4.53; N, 1.29. Found: C, 67.22; H, 4.56; N, 1.30%. ^1H NMR (δ ppm): 8.58 (dd, 7.2 Hz, 1 H), 7.58 (dd, 6.8 Hz, 1 H), 7.28 (td, 7.4 Hz, 1 H), 7.22 (td, 7.6 Hz, 1 H), 7.06–7.30 (br.m, PPh_3). $^{31}\text{P}\{^1\text{H}\}$ NMR (δ ppm): 49.62 (s, PPh_3), and 44.78 (s, PPh_3). IR (KBr pellet, cm^{-1}): 1640 (s), 1582 (s), 1478 (s), 1426 (s), 1368 (m), 1174 (m), 1127 (s), 1086 (m), 746 (m), 695 (s), 514 (s), 288 $\nu(\text{Ru}-\text{Cl})$. UV–Vis. [λ_{max} , nm (ϵ): 437 (1280), 357 (14 200), 316 (38 600), 242 (39 200).

2.2.7. Synthesis of $[\text{Ru}(\text{CO})\text{Cl}(\kappa^1\text{-P-N-PPh}_2\text{Py})_2(\text{HL}^1)]\cdot\text{CH}_2\text{Cl}_2 \mathbf{7}$

A mixture of $[\text{Ru}(\text{CO})\text{Cl}(\text{PPh}_3)_2(\text{HL}^1)]$ (0.1 g, 0.11 mmol) and PPh_2Py (0.58 g, 0.22 mmol) in dichloromethane (25 mL) were stirred at room temperature for 16 h. Slowly, it dissolved and gave a clear yellow solution. It was filtered to remove any solid impurities and concentrated to half its volume. The concentrated solution was saturated with petroleum ether (40–60 °C) and left for slow crystallization in a refrigerator. Slowly, yellow microcrystalline product separated which was filtered, washed with diethyl ether and dried *in vacuo*. Yield: 0.632 g, 77%. Microanalytical data: Anal. Calc. for $\text{C}_{39}\text{H}_{33}\text{Cl}_3\text{N}_4\text{OP}_2\text{RuS}_2$: C, 51.63; H, 3.67; N, 6.18. Found: C, 51.36; H, 3.46; N, 6.52%. ^1H NMR (δ ppm): 3.08 (s, 3H, CH_3), 8.42 [d, 1H, H6 py (P)], 7.90 (m, 1H, H3 py (P)), 7.80–7.66 [m, 4H, H2 Ph (P)], 7.24 [m, 1H, H5 py (P)], 6.68–7.25 [m, 20H, Ph (PPh_2Py)], 7.26–7.04 (br. m, 20H, (PPh_2Py)). $^{31}\text{P}\{^1\text{H}\}$ NMR (δ ppm): 48.72 (s, PPh_2Py). IR (KBr pellet, cm^{-1}): 1939 (s), 1656 (s), 1565 (s), 1486 (s), 1427 (s), 1378 (m), 1184 (m), 1127 (s), 1094 (m), 744 (m), 698 (s), 516 (s), 284 $\nu(\text{Ru}-\text{Cl})$. UV–Vis. [λ_{max} , nm (ϵ): 419 (3990), 342 (9660), 250 (34 400), 235 (38 050).

2.2.8. Synthesis of $[\text{Ru}(\kappa^1\text{-P-N-PPh}_2\text{Py})_2(\text{HL}^1)_2] \mathbf{8}$

Complex **8** was prepared following the above procedure for **7** except that $[\text{Ru}(\text{PPh}_3)_2(\text{HL}^1)_2]$ (0.1 g, 0.11 mmol) was used in place of $[\text{RuCl}(\text{CO})(\text{PPh}_3)_2(\text{HL}^1)]$. It isolated as an orange crystalline solid. Yield: 0.731 g, 74%. Microanalytical data: Anal. Calc. for $\text{C}_{40}\text{H}_{34}\text{N}_6\text{P}_2\text{RuS}_4$: C, 53.98; H, 3.85; N, 9.44. Found: C, 53.96; H, 8.84; N, 9.42%. ^1H NMR (δ ppm): 2.48 (s, 3H, CH_3), 8.38 [d, 1H, H6 py (P)], 7.94 [m, 1H, H3 py (P)], 7.88–7.82 [m, 4H, H2 Ph (P)], 7.18 [m, 1H, H5 py (P)], 6.72–7.32 [m, 20H, Ph (PPh_2Py)]. $^{31}\text{P}\{^1\text{H}\}$ NMR (δ ppm): 54.34 (s, PPh_2Py). IR (KBr pellet, cm^{-1}): 1654 (s), 1535 (s), 1446 (s), 1436 (s), 1376 (m), 1174 (m), 1128 (s), 1096 (m), 748 (m), 694 (s), 512 (s). UV–Vis. [λ_{max} , nm (ϵ): 412 (3690), 338 (9240), 244 (32 400).

2.3. X-ray crystallography

2.3.1. Details of single crystal X-ray diffraction study

Crystals suitable for single X-ray diffraction analyses for **1**, **2**, **4** and **7** were obtained from CH_2Cl_2 /petroleum ether (40–60 °C) at room temperature by the slow diffusion method. Preliminary data on space group and unit cell dimensions as well as intensity data were collected on an OXFORD DIFFRACTION XCALIBUR-S' diffractometer using graphite-monochromatized Mo K α radiation. The structures were solved by direct methods and refined by SHELXL-97.[30] Non-hydrogen atoms were refined with anisotropic

thermal parameters. All the hydrogen atoms were geometrically fixed and allowed to refine using a riding model. The computer program PLATON was used for analyzing interaction and stacking distances [31].

2.3.2. Selected crystallographic data of the complexes

Complex 1. Formula = $\text{C}_{41}\text{H}_{35}\text{Cl}_3\text{N}_2\text{OP}_2\text{RuS}_2$, Mr = 905.19, Triclinic space group $P\bar{1}$, $a = 11.397(3)$, $b = 13.346(3)$, $c = 13.889(4)$, $\alpha = 80.022$, $\beta = 70.532$, $\gamma = 85.262$, $V = 1961.0(9)$, $Z = 2$, $D_c = 1.533$, $\mu = 0.828$, T (K) = 120(2), $\lambda = 0.71073$, Reflections collected/unique 15 543/6865 [$R_{\text{int}} = 0.0210$], R (all) = 0.0398, $R(I > 2\sigma(I)) = 0.0307$, $wR_2 = 0.0883$, $wR_2 [I > 2\sigma(I)] = 0.0864$, GOF = 1.074.

Complex 2. Formula = $\text{C}_{43}\text{H}_{37}\text{Cl}_3\text{NO}_4\text{P}_2\text{RuS}_2$, Mr = 965.27, triclinic space group $P\bar{1}$, $a = 9.2816(3)$, $b = 11.4133(3)$, $c = 22.1580(7)$, $\alpha = 80.765(2)$, $\beta = 78.780(2)$, $\gamma = 69.176(2)$, $V = 2141.32(12)$, $Z = 2$, $D_c = 1.490$, $\mu = 0.647$, T (K) = 120(2), $\lambda = 0.71073$, Reflections collected/unique 15 773/7523 [$R_{\text{int}} = 0.0397$], R (all) = 0.1066, $R(I > 2\sigma(I)) = 0.0777$, $wR_2 = 0.2372$, $wR_2 [I > 2\sigma(I)] = 0.2237$, GOF = 1.002.

Complex 4. Formula = $\text{C}_{42}\text{H}_{36}\text{N}_4\text{P}_2\text{RuS}_4$, Mr = 888.00, Monoclinic space group $C2/c$, $a = 35.8089(8)$, $b = 11.5091(2)$, $c = 21.0986(5)$, $\beta = 100.9212$, $V = 8537.8(3)$, $Z = 8$, $D_c = 1.382$, $\mu = 0.672$, T (K) = 120(2), $\lambda = 0.71073$, Reflections collected/unique 30 552/7515 [$R_{\text{int}} = 0.0572$], R (all) = 0.0657, $R(I > 2\sigma(I)) = 0.0387$, $wR_2 = 0.1323$, $wR_2 [I > 2\sigma(I)] = 0.1276$, GOF = 1.019.

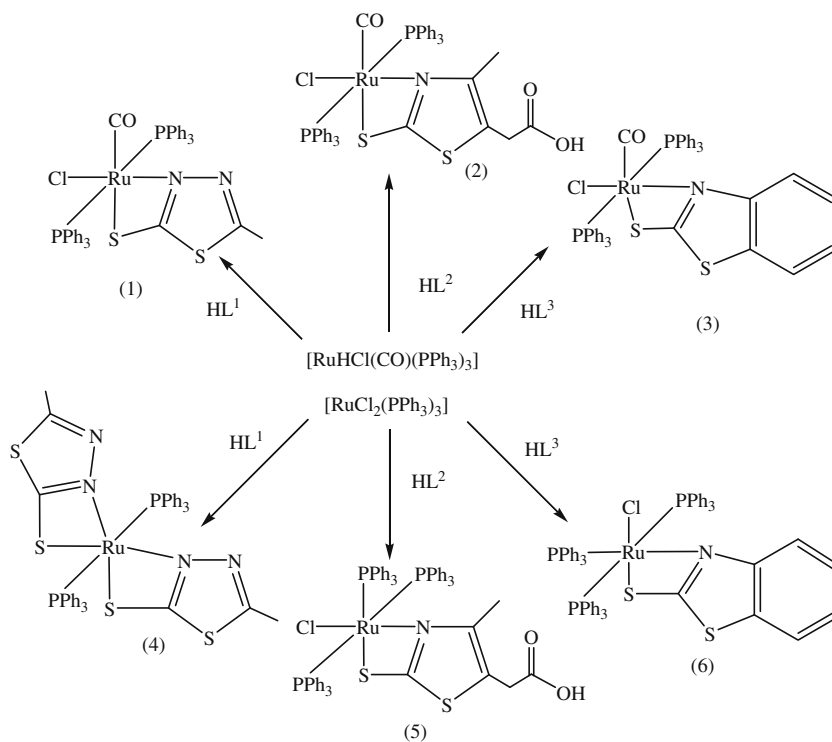
Complex 7. Formula = $\text{C}_{39}\text{H}_{33}\text{Cl}_3\text{N}_4\text{OP}_2\text{RuS}_2$, Mr = 907.19, triclinic space group $P\bar{1}$, $a = 11.472(5)$, $b = 13.606(5)$, $c = 14.003(5)$, $\alpha = 80.390(5)$, $\beta = 70.187(5)$, $\gamma = 85.134(5)$, $V = 2026.5(14)$, $Z = 2$, $D_c = 1.454$, $\mu = 0.800$, T (K) = 293, $\lambda = 0.71073$, Reflections collected/unique 28 123/9409 [$R_{\text{int}} = 0.0220$], R (all) = 0.0641, $R(I > 2\sigma(I)) = 0.0481$, $wR_2 = 0.1537$, $wR_2 [I > 2\sigma(I)] = 0.1467$, GOF = 1.146.

3. Results and discussion

Reactions of the ruthenium complexes $[\text{RuH}(\text{CO})\text{Cl}(\text{PPh}_3)_3]$ and $[\text{RuCl}_2(\text{PPh}_3)_3]$ with mercapto-functionalised thiadiazoles 2-mercapto-5-methyl-1,3,5-thiadiazole (HL^1), 2-mercapto-4-methyl-5-thiazoleacetic acid (HL^2), 2-mercaptobenzothiazole (HL^3) in methanol under refluxing conditions afforded *N,S*-bonded neutral complexes with the general formulations $[\text{Ru}(\text{CO})\text{Cl}(\text{PPh}_3)_2(\text{HL})]$ ($\text{HL} = \text{HL}^1$, **1**; $\text{HL} = \text{HL}^2$, **2**; $\text{HL} = \text{HL}^3$, **3**), $[\text{Ru}(\text{PPh}_3)_2(\text{HL}^1)_2]$ **4** and $[\text{RuCl}(\text{PPh}_3)_3(\text{HL})]$ ($\text{HL} = \text{HL}^2$, **5**; $\text{HL} = \text{HL}^3$, **6**), respectively in appreciably good yields. Formation of complexes **1–6** involves replacement of the coordinated hydride and one PPh_3 from $[\text{RuH}(\text{CO})\text{Cl}(\text{PPh}_3)_3]$ (**1–3**) and the chloro-group and one PPh_3 from $[\text{RuCl}_2(\text{PPh}_3)_3]$ (**4–6**) by *N,S*-donor sites after deprotonation from the respective ligands. A simple scheme showing syntheses of the complexes **1–6** is depicted in Scheme 3.

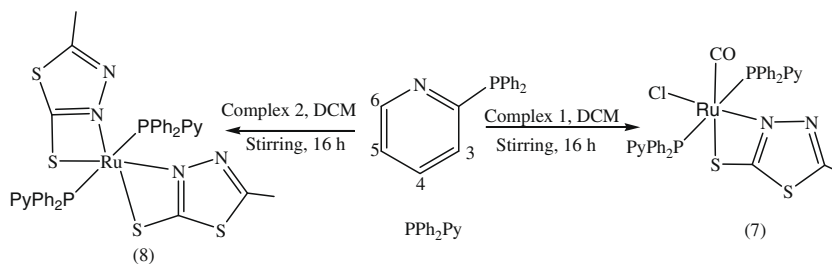
Complexes **1** and **4** reacted with hetero-difunctional ligand PPh_2Py possessing both the “soft” phosphorus and “hard” nitrogen donor sites to afford $\kappa^1\text{-P}$ coordinated neutral complexes $[\text{RuCl}(\text{CO})(\kappa^1\text{-P-PPh}_2\text{Py})_2(\text{HL}^1)]$ (**7**) and $[\text{Ru}(\kappa^1\text{-P-PPh}_2\text{Py})_2(\text{HL}^1)_2]$ (**8**). Interestingly both the coordinated PPh_3 in **1** and **4** were replaced by PPh_2Py , suggesting higher basicity of the latter in comparison to the former. Synthesis of the complexes **7** and **8** are shown in Scheme 4.

The complexes (**1–8**) are air-stable, non-hygroscopic crystalline solids soluble in halogenated solvents like dichloromethane, chloroform, insoluble in benzene, hexane, *n*-pentane, diethyl ether and petroleum ether. Characterization of the complexes have been achieved by standard spectroscopic techniques (IR, ^1H and $^{31}\text{P}\{^1\text{H}\}$ NMR, electronic spectral, and electrochemical studies) as well as elemental analyses. All the complexes gave satisfactory elemental analyses. Analytical and spectral data of these complexes corresponded to mononuclear complexes in which the ligands



HL¹ = 2-mercapto-5-methyl-1,3,5-thiadiazol, HL² = 2-mercapto-4-methyl-5-thiazoleacetic acid, HL³ = 2-mercaptobenzothiazole. Reaction conditions = methanol, reflux, 8 h

Scheme 3.



Scheme 4.

(HL¹–HL³) are bonded to metal centre through both the *S,N*-donor sites.

Formation of **1–8** has been supported by infra red spectral studies. Bands associated with $\nu(\text{C}=\text{N})$, $\nu(\text{C}=\text{S})$ and $\nu(\text{C}=\text{O})$ in the IR spectra of complexes **1–3** and **7** (~ 1433 , 1131 , 1927 cm^{-1} , **1**; 1430 , 1130 , 1930 cm^{-1} , **2**; 1435 , 1131 , 1927 cm^{-1} , **3** and 1427 , 1127 , 1939 cm^{-1} , **7**) displayed appreciable shifts in comparison to uncoordinated ligands (HL¹–HL³) and the precursor complex. Shifting in the position of bands suggested linkage of respective ligands to the metal centre. Similarly, bands associated with $\nu(\text{C}=\text{N})$ and $\nu(\text{C}=\text{S})$ were also displayed in the infra red spectra of **4**, **5**, **6**, and **8** [~ 1432 and 1136 cm^{-1} , **4**; 1429 and 1128 cm^{-1} , **5**; 1426 and 1127 cm^{-1} , **6**; 1436 and 1128 cm^{-1} , **8**]. Shift in the position of these bands in comparison to the respective ligands suggested their interaction with the metal centre.

3.1. ¹H and ³¹P{¹H} NMR spectral studies

¹H and ³¹P{¹H} NMR spectral data summarized in the experimental section strongly supported coordination of the ligands

HL¹–HL³ after deprotonation to ruthenium in neutral chelating mode. An interesting feature of ¹H NMR spectra of the complexes **1–6** is absence of resonances associated with S–H protons in the aliphatic region ($\sim 4.5\text{ ppm}$). Absence of this signal suggested that exocyclic sulfur from HL¹–HL³ along-with nitrogen donor atoms are involved in coordination with metal centre ruthenium. The aromatic protons of the coordinated triphenylphosphine resonated as broad multiplets at $\sim \delta 7.02$ – 7.38 ppm . ¹H NMR spectra of **1**, **4**, **7** and **8** exhibited singlets at $\delta 2.50$, 2.38 , $\delta 3.08$ and 2.48 ppm , respectively, assignable to the chemically equivalent methyl protons. These signals exhibited downfield shift in comparison to the uncoordinated HL¹ ($\delta 2.35\text{ ppm}$) and may be attributed to the linkage of HL¹ to metal centre ruthenium. ¹H NMR spectra of **3** and **6** displayed signals associated with coordinated HL³ at 8.61 (dd, 7.6 Hz , 1 H), 7.67 (dd, 7.8 Hz , 1 H), 7.33 (td, 7.8 Hz , 1 H), 7.24 (td, 7.6 Hz , 1 H). The down field shift in the position of signals suggested coordination of HL³ to the metal centre through both S, and N donor sites.

³¹P{¹H} NMR spectra of the complexes **1** and **4** displayed singlets at $\delta 40.72$ and $\delta 42.24\text{ ppm}$ assignable to ³¹P nuclei of the coor-

dinated triphenylphosphine. Further, the presence of a singlet suggested that both the ^{31}P nuclei in these complexes are *trans* disposed. ^{31}P in the complexes **7** and **8** resonated at δ 48.72 and 54.34 ppm, respectively. It exhibited a downfield shift in comparison to their precursors **1** and **4**. This shift may be attributed to the presence of strong donor PPh_2Py (donor ability increases in the order $\text{PPh}_3 < \text{PPh}_2\text{Py} < \text{PPhPy}_2 < \text{PPy}_3$) in comparison to PPh_3 . The ^{31}P nuclei in **3** and **6** resonated as singlets at δ 39.85 and δ 49.62, 44.78 ppm. One can see that the complex **6** exhibited two singlets owing to presence of both *cis* and *trans* phosphines ligands in this complex.

3.2. Electronic spectral studies

Electronic absorption spectra of the complexes **1–8** were acquired in dichloromethane (10^{-4} M) at room temperature and resulting data is summarized in the experimental section and spectra of **1**, **2**, **5** and **7** is depicted in Fig. 1. Complexes **1–8** displayed intense transitions in the UV–Vis region. Analogous general trend has been observed in the electronic absorption spectra of all the complexes under study. On the basis of its intensity and position lowest energy absorption bands in the visible region at \sim 485–437 and 409–357 nm have been tentatively assigned to $\text{M}_{\text{d}\pi \rightarrow \text{L}^*}$ metal to ligand charge transfer transitions (MLCT). The bands in high-energy side at \sim 235–260 nm have been assigned to intra-ligand $\pi \rightarrow \pi^*/n \rightarrow \pi^*$ transitions. [32–36] One can see that coordination of the ligands through both S and N donor sites resulted to a blue shift in the position of $\text{M}_{\text{d}\pi \rightarrow \text{L}^*}$ transitions. It may be attributed to the formation of strained four membered chelate complexes.

3.3. Electrochemistry

Electrochemical properties of **1**, **4**, and **7** have been studied by cyclic voltammetry in dichloromethane using 0.1 M tetrabutylammonium perchlorate (TBAP) as supporting electrolyte. Potential of the Fc/Fc^+ couple under the experimental conditions was 0.10 V (80 mv) vs. Ag/Ag^+ . Representative voltammogram for **1** is depicted in Fig. 2. Complexes **1**, **4** and **7** in its cyclic voltammogram exhibited an oxidative response at 0.73 (74), 0.38 (54) and 0.78 (64) V, respectively which has been assigned to $\text{Ru}^{\text{II/III}}$ oxidations. This oxidation is reversible and characterized by a peak-to-peak separation (ΔE_p) of \sim 100 mV and the anodic peak current (i_{pa}) is almost equal to the cathodic peak current (i_{pc}) expected for a reversible one elec-

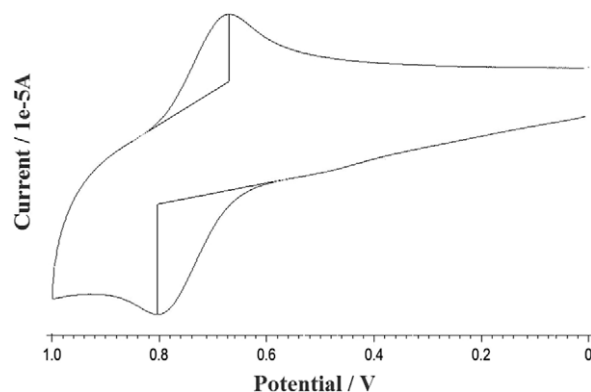


Fig. 2. Cyclic voltammogram of complex **1**.

tron-transfer process. It is observable that complexes **1** and **7** exhibited higher oxidation potential in comparison to **4**. It may be attributed to the presence of an additional π -acceptor ligand (CO) in **1** and **7**. Similar observation have been made in other complexes $\text{RuCl}_2(\text{CO})(\text{PR}_3)_3$ and $\text{RuCl}_2(\text{CO})_2(\text{PR}_3)_2$ [37]. As expected, additional π -acceptors present in the carbonyl complexes leads to higher oxidation potential.

3.4. X-ray crystallography

Structure of the complexes **1**, **2**, **4**, and **7** have been determined crystallographically. Mercury views at 30% thermal ellipsoid probability along-with atom numbering scheme is shown in Figs. 3–6. Details about data collection, solution and refinement are summarized in Section 2 and important geometrical parameters are summarized below the respective figures. Molecular structure of **1**, **2** and **7** displayed distorted octahedral geometry about the ruthenium, which is completed by N(1) and S(1) from mercapto-thiadiazoles ($\text{HL}^1\text{--HL}^2$), P(1) and P(2) from PPh_3 (**1** and **2**), or PPh_2Py (**7**), carbonyl carbon [C(1), **1**; C(40), **2** and C(6), **7**] and Cl(1). In complex **4**, it is completed by N(1), N(2), S(1) and S(2) from the mercapto-thiadiazoles (HL^1) and P(1) and P(2) from the coordinated PPh_3 . The N(1)–Ru(1)–S(1) angles are $66.8(6)^\circ$, $73.1(19)^\circ$ and $66.07(11)^\circ$, respectively in **1**, **2** and **7**, while in complex **4**, the angles N(1)–Ru(1)–S(2) and N(3)–Ru(1)–S(4) are essentially

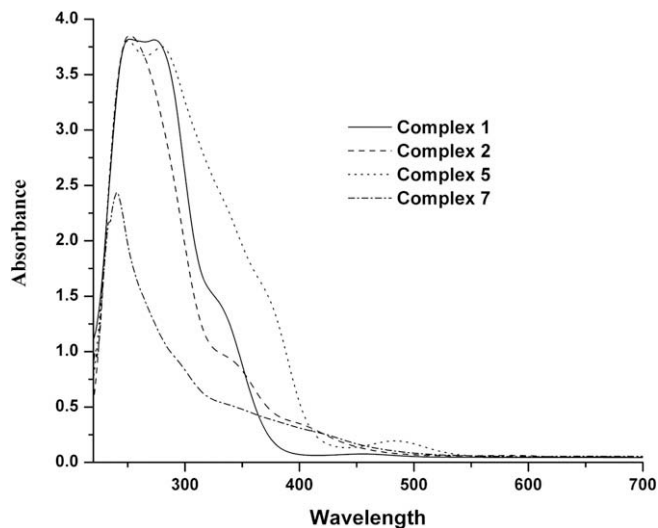


Fig. 1. UV–Visible spectra of complexes **1**, **2**, **5** and **7**.

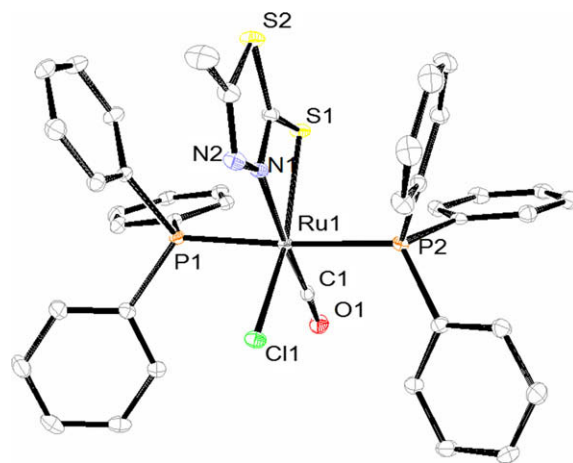


Fig. 3. Molecular structure of the complex **1** and selected bond lengths (Å) and angles ($^\circ$): Ru1–C1 1.850(3), Ru1–N1 2.154(2), Ru1–P1 2.3806(11), Ru1–P2 2.3880(11), Ru1–Cl1 2.3896(9), Ru1–S1 2.4457(9), S1–C2 1.724(3), N1–Ru1–C1 172.8(10), C1–Ru1–P1 89.1(10), C1–Ru1–P2 90.7(10), N1–Ru1–P1 90.1(7), N1–Ru1–P2 89.5(7), P1–Ru1–P2 175.6(3), N1–Ru1–S1 66.8(6).

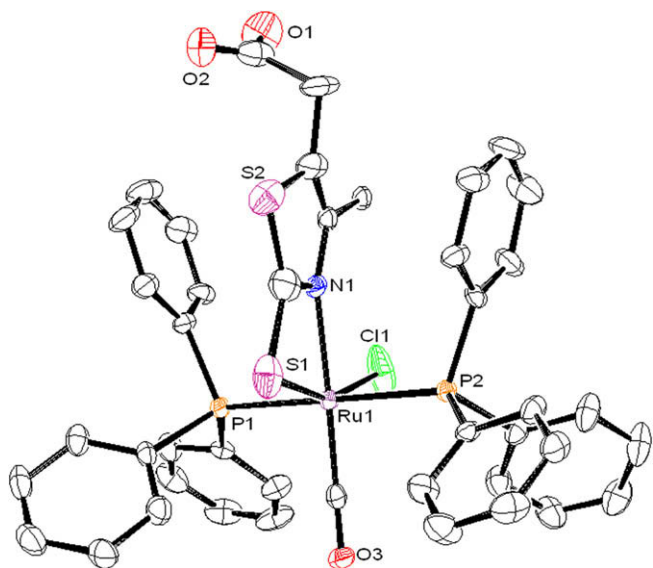


Fig. 4. Molecular structure of the complex **2** and selected bond length (Å) and angles (°): Ru1–C6 1.827(7), Ru1–N1 2.162(5), Ru1–P1 2.3638(18), Ru1–P2 2.3713(18), Ru1–S1 2.413(3), Ru1–Cl1 2.462(3), S1–C2 1.822(12), N1–Ru1–C6 175.3(3), C6–Ru1–P1 90.7(2), C6–Ru1–P2 89.5(2), N1–Ru1–P1 90.2(15), N1–Ru1–P2 89.7(15), P1–Ru1–P2 176.9(7), N1–Ru1–S1 73.1(19).

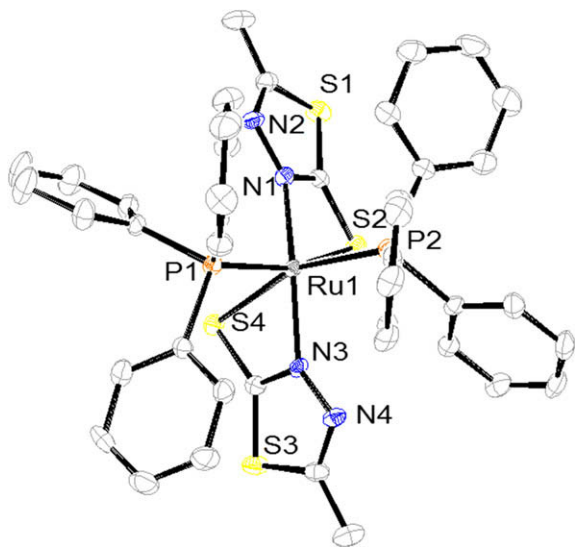


Fig. 5. Molecular structure of the complex **4** and selected bond length (Å) and angles (°): Ru1–N1 2.084(4), Ru1–N3 2.069(4), Ru1–P1 2.2940(14), Ru1–P2 2.2838(14), Ru1–S2 2.5456(14), Ru1–S4 2.5466(14), N1–Ru1–P1 98.5(12), N1–Ru1–P2 94.4(12), N3–Ru1–P1 92.3(12), N3–Ru1–P2 95.5(12), P1–Ru1–P2 103.8(5), N1–Ru1–S2 66.03(12), N1–Ru1–S4 101.1(12), N3–Ru1–N1 162.9(17), P1–Ru1–S2 162.9(5), P2–Ru1–S2 85.3(5), P1–Ru1–S4 87.1(5), P2–Ru1–S4 159.4 (5).

equal and 66.03(12)° and 66.1(12)°, respectively. It suggested inward bending of mercapto-thiadiazole moiety towards metal centre and smaller value of this angle in comparison to ideal value of 90° is probably source of the observed distortion.

The angles P(1)–Ru–P(2) in **1**, **2** and **4** are 175.6(3)°, 176.9(7)°, and 103.8(5)°, respectively and associated P(1)–Ru(01)–P(2) angle in **7** is 174.6(4)°. The P–Ru–P angles suggested that triphenylphosphine ligands are *trans* disposed in **1**, **2** and **7**, while it adopted a *cis* arrangement in **4**. The Ru(1)–P(1) and Ru(1)–P(2) bond distances are 2.3806(11) and 2.3880(11) Å in **1**, while it is 2.2940(14) and 2.2838(14) Å in **4**. These are essentially equivalent and comparable to the values reported in other related complexes [38–41]. The

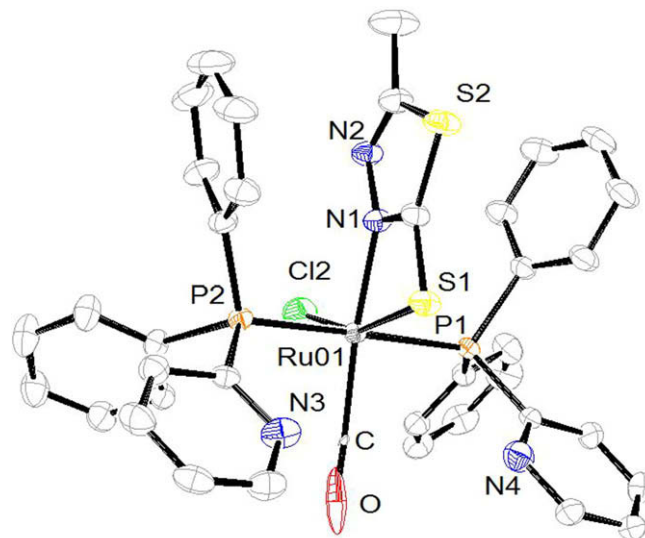


Fig. 6. Molecular structure of complex **7** and selected bond length (Å) and angles (°): Ru01–C_≡O 2.240(4), Ru01–N1 2.117(4), Ru01–P1 2.3804(14), Ru01–P2 2.3851(15), Ru01–Cl2 2.406(2), Ru01–S1 2.4968(14), S1–C35 1.719(5), N1–Ru01–C_≡O 173.6(6), P1–Ru01–C_≡O 88.9(5), P2–Ru01–C_≡O 89.9(5), N1–Ru01–P1 90.6(12), N1–Ru01–P2 89.8(12), P1–Ru01–P2 174.6(4), N1–Ru01–S1 66.07(11).

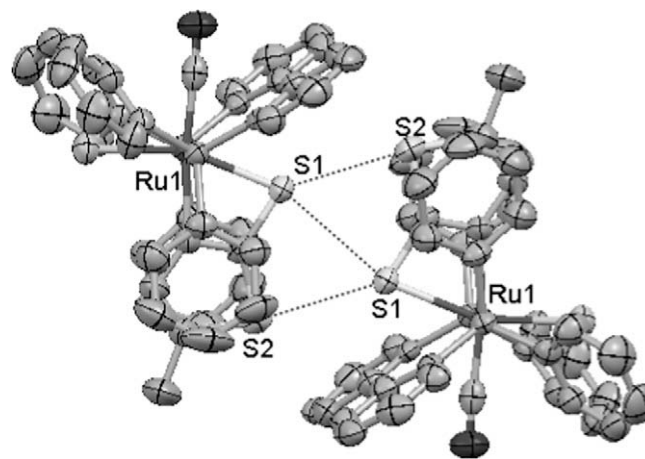


Fig. 7. Intermolecular association of coordinated 2-mercapto-5-methyl-1,3,5-thiadiazol (HL¹) ligands in the crystal of complex **1**. Angles between the planes defined by S(2)–S(1)–S(1) 55.75°, C(2)–S(2)–S(1) 86.29°, C(2)–S(1)–S(1) 82.26°.

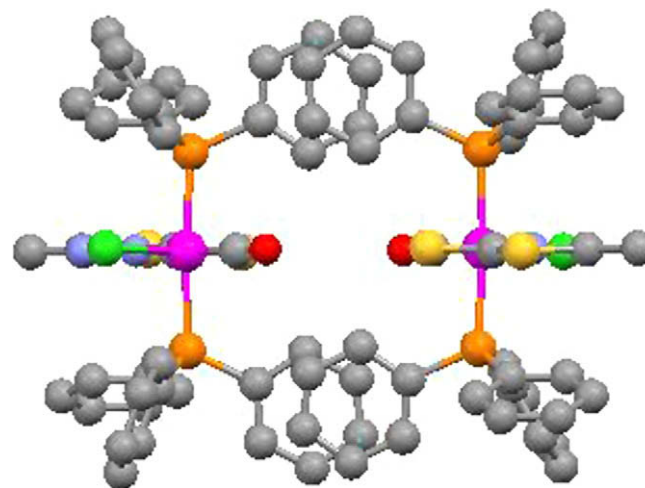


Fig. 8. Face-to-face π–π interaction leading to supramolecular motif in complex **1**.

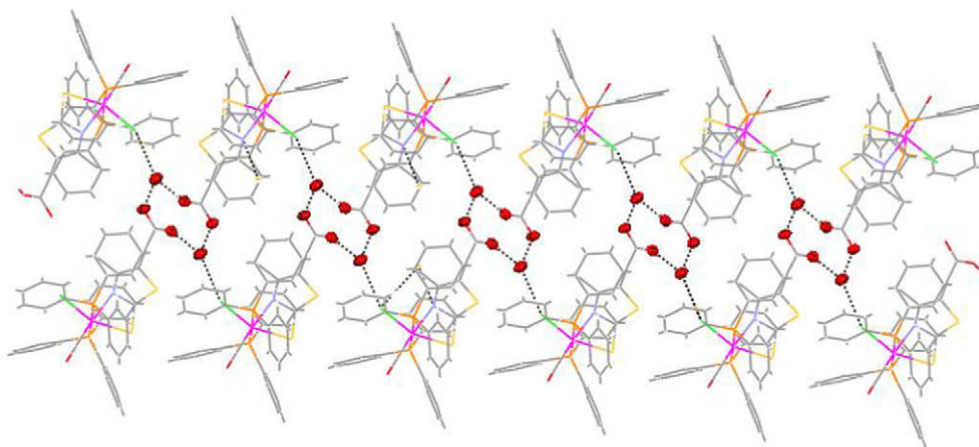


Fig. 9. Hydrogen-bonding intermolecular interactions between carboxylate oxygen and water molecules leading to regular hexamer motif in **6**.

ruthenium to carbonyl carbon Ru(1)–C(1) bond distances are 1.850(3), 1.827(7) and 2.240(4) Å, respectively in **1**, **2** and **7**. It falls in the range for Ru–C carbonyl bond lengths [40,42,43]. The Ru(1)–S(1) bond distances are 2.4457(9), 2.413(3) and 2.4968(14) Å, in **1**, **2**, and **7**, while Ru(1)–S(2) and Ru(1)–S(4) bond distances in **4** are 2.5456(14) and 2.5466(14) Å. These are normal for Ru(II)–S bond distances [41–43]. The S–C bond distances in **1**, **2** and **7** are in the range of 1.82–1.71 Å [S(1)–C(2) 1.724(3), **1**; S(1)–C(2) 1.822(12), **2**; S(1)–C(35) 1.719(5) Å, **7**] and it is 1.716(6) Å in **4**. It is well established that the S–C distances in thiol form falls in the range of 1.83–1.70 Å [41]. Therefore, coordinated mercapto groups in **1**, **2**, **4**, and **7** are present in thiol forms.

It is interesting to note that two distinct molecules in the asymmetric unit of complex **1** are apparently linked intermolecularly by the unusual arrangement of two sulfur atoms from 2-mercapto-5-methyl-1,3,5-thiadiazole (Fig. 7). The secondary bonding is clearly weak [S(1)⋯S(1) 3.461, S(1)⋯S(2) 3.461 Å; covalent radii sums S–S 2.04 Å], however it should be noted that the complex is sterically cluttered and this may be limiting the interaction. Intermolecular interactions in the solid state between sulfur and nitrogen or sulfur in sulfur–nitrogen containing compounds are uncommon and in particular, thiadiazoles as a class often show this feature, however it is less common in coordination complexes. Weak interaction studies in **1** shows face-to-face π – π (3.645 Å) interactions between two distinct molecules leading to supramolecular motif shown in Fig. 8. Further, complex **6** displayed weak intermolecular association between free carboxylate and water molecules leading to regular hexamer motif (Fig. 9).

4. Conclusion

In summary, in this work we have presented synthesis and characterization of mononuclear ruthenium(II) complexes based on 2-mercapto-5-methyl-1,3,5-thiadiazole, 2-mercapto-4-methyl-5-thiazoleacetic acid, and 2-mercaptobenzothiazole. It has been demonstrated that the thiadiazole ligands interacted with the ruthenium through S and N donor atoms in their thiol forms leading to distorted octahedral complexes. In the complexes under investigation the mercapto-functionalised thiadiazoles are bonded to ruthenium in neutral chelating mode. Structural studies revealed that complex **1** involves rare S–S interactions.

Acknowledgements

We gratefully acknowledge financial support from the Department of Science and Technology, Ministry of Science and Technol-

ogy, New Delhi, India (Grant No. SR/SI/IC-15/2007). Also, we are thankful to Prof. P. Mathur, In-charge, National Single Crystal X-ray Diffraction Facility, Indian Institute of Technology, Mumbai for providing single crystal X-ray data.

Appendix A. Supplementary material

CCDC 753774, 753775, 753776, and 753777 contains the supplementary crystallographic data for complexes **1**, **2**, **4**, and **7**. These data can be obtained free of charge from The Cambridge Crystallographic Data Centre via www.ccdc.cam.ac.uk/data_request/cif. Supplementary data associated with this article can be found, in the online version, at [doi:10.1016/j.jorganchem.2009.12.006](https://doi.org/10.1016/j.jorganchem.2009.12.006).

References

- [1] I.S. Oae, Organic Sulphur Chemistry: Structure and Mechanism, CRC Press Inc., Florida, 1992.
- [2] A. Millar, B. Krebs, Sulphur, its Significance for Chemistry, for Geology Biology, Cosmospere and Technology, Elsevier, Amsterdam, 1989.
- [3] E.S. Raper, Coord. Chem. Rev. 165 (1997) 475, and references therein.
- [4] E. Shouji, D.A. Buttry, J. Phys. Chem. B 102 (1998) 1444.
- [5] G. Kornis, A.R. Katritzky, C.W. Rees (Eds.), 1,3,4-Thiadiazoles, Comprehensive Heterocyclic Chemistry, vol. 6, Pergamon Press, Oxford, 1984, p. 545, part 4B.
- [6] A.R. Katritzky, Z. Wang, R.J. Offerman, J. Heterocycl. Chem. 27 (1990) 139.
- [7] K. Umakoshi, T. Yamasaki, A. Fukuoka, H. Kawano, M. Ichimura, Inorg. Chem. 41 (2002) 4093, and references therein.
- [8] O. Asada, K. Umakoshi, K. Tsuge, S. Yabuuchi, Y. Sasaki, M. Onishi, Bull. Chem. Soc. Jpn. 76 (2003) 549.
- [9] P.D. Akrivos, Coord. Chem. Rev. 213 (2001) 181.
- [10] S.A.A. Zaidi, A.S. Farooqi, D.K. Varshney, V. Islam, K.S. Siddiqi, J. Inorg. Nucl. Chem. 39 (1977) 581.
- [11] M. Brezeanu, R. Olar, A. Meghea, N. Stanica, C.T. Supuran, Rev. Roum. Chim. 41 (1996) 103.
- [12] M.R. Gajendragad, U. Agarwala, Z. Anorg. Allg. Chem. 415 (1975) 84.
- [13] P. Ortega, L.R. Ver, M.E. Guzmán, Macromol. Chem. Phys. 198 (1997) 2949.
- [14] S.A.A. Zaidi, D.K. Varshney, J. Inorg. Nucl. Chem. 37 (1975) 1804.
- [15] M.R. Gajendragad, U. Agarwala, Indian J. Chem. 13 (1975) 697.
- [16] F. Hipler, S. Gil Girol, R.A. Fischer, Ch. Woll, Mat.-Wiss. u. Werkstofftech. 31 (2000) 872.
- [17] N. Oyama, T. Tatsuma, T. Sato, T. Sotomura, Nature (London) 373 (1995) 598.
- [18] H. Tannai, K. Tsuge, Y. Sasaki, O. Hatozaki, N. Oyama, Dalton Trans. (2003) 2353.
- [19] M. Gras, B. Therrien, G. Süß-Fink, P. Štepnicka, A.K. Renfrew, P.J. Dyson, J. Organomet. Chem. 693 (2008) 3419.
- [20] F.E. Hong, Y.C. Chang, R.E. Chang, C.C. Lin, S.L. Wang, F.L. Liao, J. Organomet. Chem. 588 (1999) 160.
- [21] F.E. Wood, M.M. Olamstead, J.P. Farr, A.L. Balch, Inorg. Chim. Acta 97 (1985) 77.
- [22] P. Kumar, A.K. Singh, D.S. Pandey, J. Organomet. Chem. 694 (2009) 3643.
- [23] D.D. Perrin, W.L.F. Armango, D.R. Perrin, Purification of Laboratory Chemicals, Pergamon, Oxford, UK, 1986.
- [24] P.S. Hallman, T.A. Stephenson, G. Wilkinson, Inorg. Synth. 12 (1970) 238.
- [25] B.P. Sullivan, J.M. Calvert, T.J. Meyer, Inorg. Chem. 19 (1980) 1404.

- [26] G.M. Sheldrick, *SHELX-97: Programme for the Solution and Refinement of Crystal Structures*, University of Göttingen, Germany, 1997.
- [27] A.L. Spek, *Acta Crystallogr.* 46 (1990) C31.
- [28] R.M. Berger, D.D. Ellis II, *Inorg. Chim. Acta* 241 (1996) 1.
- [29] P. Paul, B. Tyagi, M.M. Bhadbhade, E. Suresh, *J. Chem. Soc., Dalton Trans.* (1997) 2273.
- [30] R.M. Berger, J.R. Holcombe, *Inorg. Chim. Acta* 232 (1995) 217.
- [31] P. Kopel, Z. Travnicsek, L. Kvitek, R. Panchartkova, M. Biler, M. Marek, M. Nadvornik, *Polyhedron* 18 (1999) 1779.
- [32] S. Kar, T.A. Millar, S. Chakraborty, B. Sarkar, B. Pradhan, R.K. Singh, T. Kunda, M.D. Ward, G.K. Lahiri, *Dalton Trans.* (2003) 2591.
- [33] E.B. Milosavljevic, Lj. Solujic, D.W. Krassowski, J.H. Nelson, *J. Organomet. Chem.* 352 (1988) 177.
- [34] J.C. Mc Conway, A.C. Skapski, L. Phillips, R.J. Young, G. Wilkinson, *J. Chem. Soc., Chem. Commun.* (1974) 327.
- [35] I. de Los Rios, M.J. Tenorio, M.A.J. Tenorio, M.C. Puerta, P. Valerga, *J. Organomet. Chem.* 525 (1996) 57.
- [36] P. Ghosh, A. Chakravorty, *Inorg. Chem.* 36 (1997) 64.
- [37] O.S. Sisodia, A.N. Sahay, D.S. Pandey, U.C. Agrawala, N.K. Jha, P. Sharma, A. Toscano, A. Cabrera, *J. Organomet. Chem.* 560 (1998) 35.
- [38] M. Chandra, A.N. Sahay, D.S. Pandey, M.C. Puerta, P. Valerga, *J. Organomet. Chem.* 648 (2002) 39.
- [39] M.F. McGuiggan, L.H. Pignolet, *Inorg. Chem.* 21 (1982) 2523.
- [40] A. Sahajpal, S.D. Robinson, M.A. Mazid, M. Motevalli, M.B. Hursthouse, *J. Chem. Soc., Dalton Trans.* (1990) 2119.
- [41] M. El-khateeb, K. Damer, H. Görls, W. Weigand, *J. Organomet. Chem.* 692 (2007) 2227.
- [42] J. Mola, I. Romero, M. Rodriguez, F. Bozoglian, A. Poater, M. Sola, T. Parella, J. Benet-Buchholz, X. Fontrodona, A. Llobet, *Inorg. Chem.* 46 (2007) 10707.
- [43] D. Sukanya, M.R. Evans, M. Zeller, K. Natarajan, *Polyhedron* 26 (2007) 4314.